Journal of Neurochemistry

JOURNAL OF NEUROCHEMISTRY | 2020 | 152 | 650–662 doi: 10.1111/jnc.14897

ORIGINAL ARTICLE

Distinct gradients of various neurotransmitter markers in caudate nucleus and putamen of the human brain

Heide Hörtnagl*, Christian Pifl†, Erik Hörtnagl‡, Angelika Reiner§ and Günther Sperk*

*Department of Pharmacology, Innsbruck Medical University, Innsbruck, Austria
†Centre for Brain Research, Medical University of Vienna, Vienna, Austria
‡ipsum, interkultureller Kunstverein, Müllerstr. 28, Innsbruck, Austria
§Department of Pathology, Danube Hospital, Vienna, Austria

Abstract

The caudate nucleus (CN) and the putamen (PUT) as parts of the human striatum are distinguished by a marked heterogeneity in functional, anatomical, and neurochemical patterns. Our study aimed to document in detail the regional diversity in the distribution of dopamine (DA), serotonin, γ-aminobuturic acid, and choline acetyltransferase within the CN and PUT. For this purpose we dissected the CN as well as the PUT of 12 *post-mortem* brains of human subjects with no evidence of neurological and psychiatric disorders (38–81 years old) into about 80 tissue parts. We then investigated rostro-caudal, dorso-ventral, and medio-lateral gradients of these neurotransmitter markers. All parameters revealed higher levels, turnover rates, or activities in the PUT than in the CN. Within the PUT, DA levels increased continuously from rostral to caudal. In contrast, the lowest molar ratio of homovanillic acid to DA, a marker of DA turnover, coincided with highest DA levels in the caudal PUT, the part of the striatum with the highest loss of DA in Parkinson's disease (N. Engl. J. Med., 318, 1988, 876). Highest DA concentrations were found in the most central areas both in the PUT and CN. We observed an age-dependent loss of DA in the PUT and CN that did not correspond to the loss described for Parkinson's disease indicating different mechanisms inducing the deficit of DA. Our data demonstrate a marked heterogeneity in the anatomical distribution of neurotransmitter markers in the human dorsal striatum indicating anatomical and functional diversity within this brain structure.

Keywords: caudate nucleus, dopamine, human brain, Parkinson's disease, putamen, serotonin.
J. Neurochem. (2020) **152**, 650–662.

Read the Editorial Highlight for this article on page 623.

In the human brain the dorsal striatum is functionally related to a variety of higher brain functions and receives inputs from multiple cortical regions. It is subdivided into the caudate nucleus (CN) and the putamen (PUT), not including the nucleus accumbens. The rich and diverse functional and anatomical connectivity patterns of the striatum suggest the existence of distinguishable and potentially functionally relevant anatomical subunits within both of its parts that should be characterized by specific local microstructural traits such as cytoarchitecture or distribution of neurotransmitters and their receptors (Kotz *et al.* 2013). Based on the heterogenous distribution of acetylcholinesterase in the human striatum a striosome-matrix compartmentalization has been highlighted (Graybiel & Ragsdale 1978, Graybiel 1990; Crittenden and Graybiel 2011). According to Johnston *et al.* (1990) the rostral striatal sections are slightly richer in striosomes (17%) than the caudal sections (9.8%), on average among species. The percentage of the human striatum occupied by the striosome compartment in the CN (14.0%)

Received June 19, 2019; revised manuscript received October 7, 2019; accepted October 10, 2019.

Address correspondence and reprint requests to Heide Hörtnagl, Department of Pharmacology, Innsbruck Medical University, Peter-Mayr-Strasse 1a, A-6020 Innsbruck, Austria. E-mail: heide.hoertnagl@i-med.ac.at

This manuscript is dedicated to Prof. Dr. Oleh Hornykiewicz on the occasion of his 93th birthday as a tribute to his outstanding contributions to the etiology and treatment of Parkinson's disease.

Abbreviations used: 5-HIAA, 5-hydroxyindoleacetic acid; 5-HT, serotonin; ac, anterior commissure; ChAT, choline acetyltransferase; CN, caudate nucleus; DA, dopamine; GABA, γ-aminobuturic acid; HVA, homovanillic acid; PUT, putamen; TH, tyrosine hydroxylase; ww, wet weight.

is significantly different from that in both the rostral PUT (29.2%) and caudal PUT (28.1%; Morigaki and Goto 2016). Beyond these differences in the fine structure of the dorsal striatum, cholinergic interneurons show a diverse distribution (Bernácer *et al.* 2007). The CN is more densely populated by cholinergic neurons than the PUT and their density increases along the antero-posterior axis of the striatum with the CN body having the highest neuronal density.

In corticostriatal pathways two strong organizational gradients exist, one in a medial-lateral orientation, the second in a rostro-caudal direction (Jarbo and Verstynen 2015; Shipp 2017). Parkes *et al.* (2017) identified a tripartite organization of the CN and PUT that comprises ventral, dorsal, and caudal subregions. These subregions show distinct cortical connectivity profiles. The finding of a rostro-caudal gradient supports functionally specialized circuits within the broader ventral-affective, dorsal-associative, and caudal-sensorimotor partitions.

In the striatum of neurologically healthy humans, dramatic differences in the distribution of components of dopaminergic neurotransmission have been described *in vivo* as well as *post-mortem*. The density of distinct classes of dopamine (DA) receptors varies across subregions of the dorsal striatum (Piggott et al., 1999; Alakurtti *et al.* 2013). According to Piggott et al. (1999) the density of DA uptake sites ([^{3}H]mazindol binding) exhibit an increasing rostro-caudal gradient in the CN, especially ventrally, whereas in the PUT the binding is more balanced. Tyrosine hydroxylase (TH) as a marker of dopaminergic nerve terminals is distributed in a non-homogenous pattern of low and high immunoreactive zones. The density of TH-labeling was significantly higher in the matrix than in the striosomes indicating that DA neurons terminate in the matrix (Morigaki and Goto 2016). Notably, striosomes of low TH immunoreactivity were more evident in the PUT than in the CN.

The diversity within the striatum is also obvious in the development of pathological changes such as Parkinson's disease. In Parkinson's disease the depletion of DA was most remarkable in the PUT particularly in its caudal portions (Kish *et al.* 1988). Similarly, the decline in DA transporter binding was most pronounced in the posterior PUT in Parkinson's disease (Wang *et al.* 2006; Hong *et al.* 2014). In Parkinsonian patients the pathological lesion was found specifically in the lateral portion of the *substantia nigra* that forms a link to the PUT (Goto *et al.* 1989). Morrish *et al.* (1996) demonstrated a 50% reduction in [18F]DOPA metabolism in the dorsal, but not in the ventral PUT in early Parkinson's disease. In Huntington's disease the caudal portion of the PUT has degenerated to a larger extent than the rostral portion in the early phase of the disease and additionally, the tail of the CN is more severely affected than the body of CN (Vonsattel and DiFiglia 1998).

This increasing evidence of high functional, anatomical and neurochemical diversities in the healthy and diseased human dorsal striatum lead us to investigate and quantify in detail the distribution of neurotransmitter markers characteristic for the dorsal striatum and to compare the distributions between CN and PUT in the healthy human brain. The aim of this study was to define detailed subregional patterns in the levels of the neurotransmitters DA and serotonin (5-HT) as parameters for aminergic innervation, their metabolites homovanillic acid (HVA), 3,4-dihydroxyphenylacetic acid (DOPAC), and 5-hydroxyindoleacetic acid (5-HIAA) as markers for the activity of the respective neurons, choline acetyltransferase (ChAT) activity as marker for cholinergic neurons and the neurotransmitter γ-aminobuturic acid (GABA), contained in interneurons and projection neurons arising from the dorsal striatum. Evidence obtained in the neostriatum of the rat indicates a distinct diversity in the distribution of monoamines and their metabolites. The highest levels of DA have been detected in dorso-rostral areas and lowest content in the ventro-caudal part (Widmann and Sperk, 1986).

Methods

Ethical approval and brain retrieval

Brains were retrieved *post-mortem* and the tissue processed according to the legislation and national guidelines at the time of retrieval. According to Austrian law it is possible to retrieve appropriate tissue samples during routine autopsies for scientific research without informed consent (see GZ 92600/0027-II/A/4/2013). The study was approved by the Ethics Committee, Medical University Vienna: EK Nr: 1353/2019; 15-05-2019.

Autopsied brains were obtained from 12 subjects with no history of neurological, psychiatric, or neuropathological disorders. The brains were obtained in the context of pathological autopsies at the Department of Pathology, University of Vienna, Austria, (by A. Reiner). The inclusion criterion was the absence of any evidence for neurological, psychiatric or neuropathological disorder. No sample size calculation to predetermine sample size and no test for outliers were performed. The study was not pre-registered.

Age, gender, *post-mortem* interval until autopsy and cause of death are summarized in Table 1. The mean age of the subjects was 60.5 ± 4.2 years. The mean *post-mortem* interval was 11.4 ± 1.9 h.

Dissection of the brains

At autopsy, brains were removed and divided into individual hemispheres by a mid-sagittal section after removing the brainstem. The hemispheres to be used for neurochemical analysis were immediately frozen at −80°C and kept at this temperature from 0.5 to 12 months until dissection. The topographical dissection was carried out by Prof. Oleh Hornykiewicz on the basis of Riley's Atlas of the Basal Ganglia, Brainstem, and Spinal Cord (Riley, 1960). Fifteen coronal slices, each 3–4 mm thick, were cut beginning at the rostral pole of the CN (coronal level −20.0 mm from anterior commissure, ac) and ending with the body of the CN (coronal level + 31.9 mm from ac, according to Mai *et al.* 1997). The slices were placed on glass plates kept at around −20°C by dry ice placed

Table 1 Information on the subjects included in the study

No.	Age (years)	Gender	*Post-mortem* Interval (h)	Cause of death
1	38	Female	< 4	Mesothelioma
2	66	Female	23	Larynx carcinoma
3	57	Female	8	Lung squamous cell carcinoma
4	70	Male	16	Tongue squamous cell carcinoma
5	81	Female	5	Cardiac failure
6	63	Female	7	Uterine corpus carcinoma
7	48	Female	18	Vulva carcinoma
8	44	Female	17	Cervix carcinoma
9	66	Male	4	Myocardial infarction
10	44	Female	11	Ovarian cancer
11	68	Male	9	Cardiac failure
12	81	Female	15	Mammary carcinoma

underneath. In 5 of the 12 brains slices 1 to 9 of the CN, and slices 3 to 12 of the PUT were dissected into dorsal, intermediate, and ventral subdivisions using a surgical scalpel. In the seven remaining brains subdivisions of slices 2 to 9 of the CN and 4–12 of the PUT were further divided into medial, intermediate and lateral parts (as schematically drawn in Fig. 4). In these brains values in the dorsal-intermediate-ventral and medial-intermediate-lateral subdivisions were recalculated by adding the values/mg wet weight (ww) of the parts multiplied by the respective weight and dividing the resulting sum by the total weight of these parts. One of the brains was used for the analysis of GABA only. Tissue specimens were immediately transferred to Eppendorf vials, weighed (ww) and put on dry ice. The average weight of the tissue specimens (as schematically drawn in Fig. 4) was e.g. in slice 7: 26.0 ± 1.3 mg in the CN (n = 63); 37.4 ± 1.9 mg in the PUT (n = 63); in slice 9: 16.8 ± 0.9 mg in the CN (n = 63); 30.5 ± 1.2 mg in the PUT (n = 63). The samples were kept at −80°C until neurochemical analysis was performed.

Neurochemical analyses

Tissue samples were homogenized by ultrasonication in N_2-saturated deionized water, 20–40 times the volume of the wet weight of the sample. Immediately after sonification an aliquot of the homogenate was added to an equal volume of 0.2 M perchloric acid containing 0.8 mM $NaHSO_3$ and centrifuged at 25.000 g for 15 min. The supernatant was used to measure DA, HVA, DOPAC, 5-HT, 5-HIAA, and GABA. The remaining aqueous homogenate was used to measure ChAT activity.

ChAT activity was measured according to Fonnum (1969) with minor modifications using substrate concentrations of 8 mM choline chloride and 0.2 mM acetyl coenzyme A (Sperk *et al.* 1983).

DA was measured by high-performance liquid chromatography (HPLC) with electrochemical detection after adsorption to alumina according to Felice *et al.* (1978) with minor modifications (Sperk *et al.* 1981). HVA, DOPAC, 5-HT and 5-HIAA were determined by HPLC with electrochemical detection as described by Sperk, 1982. GABA levels were determined by HPLC after post-column derivatization with the fluorogenic reagent *O*-phthaldialdehyde according to the method described by Schmid *et al.* (1980) using a fluorometric detector (360/450 nm).

Materials

Standards for HPLC analysis were purchased from Sigma, St Louis, MI, USA: DA (H8502), HVA (H1552), DOPAC (850217), 5-HT (H7752), 5-HIAA (H8876), and GABA (A5835). Choline chloride was obtained from Sigma (C7527), o-phtalaldehyde from Serva, Germany (Nr.32800). [^{14}C] acetyl coenzyme A (56.6 mCi/mmol) was obtained from Amersham plc, Great Britain (CFA 452). For monoamine/metabolite analysis HPLC μBondapak C-18 columns from Waters Ass., MA, USA were used. For GABA analysis a 3.1 × 250 mm column was self-packed with Aminex A9 cation exchange resin from BioRad, Hercules, CA, USA.

Data analysis

All values are expressed as the mean ± SEM. Normality of data was assessed according Shapiro–Wilk. Differences between samples obtained from slices subdivided into medial, intermediate, and lateral or into dorsal, intermediate and ventral parts were analyzed by two-way repeated measures ANOVA (Two Factor Repetition), followed by pairwise multiple comparison procedures (Holm–Sidak method). If data were non-normal, they were transformed to ranks, followed by a two-way ANOVA on the ranks. Differences between rostro-caudal slices of undivided CN or PUT were analyzed by one-way repeated measures ANOVA, again followed by pairwise multiple comparison procedures (Holm–Sidak method). Correlations between parameters were calculated by the Pearson Product Moment Correlation. These correlations were used to (i) describe the existence of a gradient along the rostro-caudal axis in lateral, ventral, and medial parts of the CN and the PUT for a given parameter (i.e., slice number versus parameter), and (ii) determine possible correlations between parameters within the different subdivisions of the CN and the PUT. A correlation was only considered significant with a p value below 0.05 after Bonferroni correction for repetitive calculations between the various parameters. The correlations were performed with the mean values of the data coming from the entire cohort.

Results

Differences in the rostro-caudal, dorso-ventral, and medio-lateral distribution of dopamine in the human putamen and caudate nucleus

We first analyzed the levels of DA in the whole slice from rostral to caudal. Two-way repeated measures ANOVA (Two Factor Repetition) followed by pairwise multiple comparison procedures (Holm–Sidak method) calculated significantly higher levels in the PUT than in the CN in slices 6 to 12 (Fig. 1). Furthermore, in the PUT we observed a clear increase in DA concentrations from rostral to caudal portions, indicated by significantly higher DA levels in slices 6 to 12 as compared to slice 3 (One Way Repeated Measures Analysis of Variance). In contrast, in the CN the initial rostral increase in DA levels was followed by a plateau and a considerable decline in the caudal portions of the nucleus, indicated by significantly higher DA levels in the

slices 4 to 9 than in slices 1, 2, and 13 to 15 (Fig. 1; for presentation of respective box-plots see Figure S1a).

Next we focused on whether a heterogeneity in the distribution of DA in the human striatum can also be found in medio-lateral as well as dorso-ventral directions. Therefore, we analyzed the DA levels of three adjacent tissue samples taken from the coronal sections in the medial to lateral or dorsal to ventral directions. In the intermediate part of the CN, we found the highest DA levels both in the medio-lateral (left panel of Fig. 2a, slices 4–6) and in the dorso-ventral directions (right panel of Fig. 2a, slices 6 and 7). In contrast, we saw the lowest DA levels in the medial part of the CN (left panel of Fig. 2a, slices 2–8). In the PUT the regional differences in DA concentrations were less pronounced although there was a tendency towards higher levels in the intermediate parts. In lateral, intermediate, and ventral

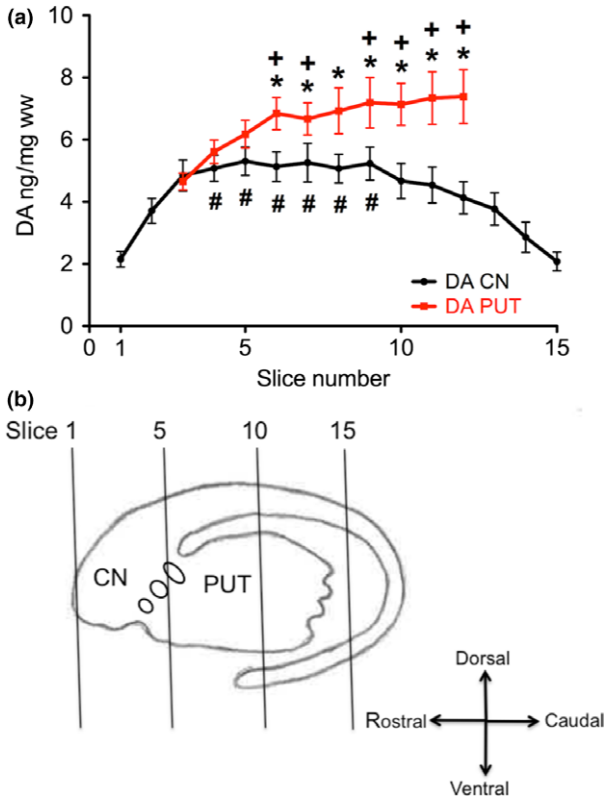

Fig. 1 Rostro-caudal gradient of DA in the human CN and PUT. (a) Coronal slice 1 represents the rostral pole of the CN (coronal level −20.0 mm from ac). Slice 15 represents the ending of the body of the CN (coronal level + 31.9 mm from ac, according to Mai et al. 1997). The concentration of DA in ng/ mg ww was calculated for the whole area of CN (black) and PUT (red) in the corresponding slice. Eleven brain hemispheres were investigated. The data are given as mean ± SEM. *$p < 0.05$ *vs.* CN; +$p < 0.05$ vs. slice 3 of PUT; #$p < 0.05$ versus slices 1 and 2 and 13 to 15 of CN (see Figure S1a for presentation of respective box-plots). (b) Schematic drawing of the dorsal striatum including the approximate location of slices 1, 5, 10, and 15.

subregions of the PUT levels of DA followed a linearly increasing rostro-caudal gradient (Fig. 3a) with levels linearly correlating with slice numbers (correlation coefficients of 0.92–0.97, $p < 0.001$) and a significantly positive slope ($p < 0.001$), whereas we detected no significant rostro-caudal gradient in medial parts. In the dorsal subdivision, DA levels increased from slices 3 to 6 and then remained at about the same level up to slice 12, being significantly higher than in slice 3 (Fig. 3a). When we subdivided the CN and PUT into nine parts per slice it became obvious that the highest DA levels were present in the center, both of the CN and of the PUT [Fig. 4a, Table S1; shown in six different representative coronal sections: −12.5 mm (slice 4), −5.8 mm (slice 6), −2.7 mm (slice 7), +1.3 mm (slice 8), +5.4 mm (slice 9), and +16.0 mm (slice 11) from ac].

Diversity of dopamine turnover in the various subregions of the human dorsal striatum

Since HVA is the main metabolite of DA in the human brain (Wilk and Stanley 1978; Kopin 1985; Ebinger *et al.* 1987) and partially reflects DA release after extra-neuronal formation, we preferentially determined this DA metabolite in our samples. In the whole slices of the CN the concentrations of HVA increased in the rostro-caudal direction with significantly higher levels in slice 4 than in slices 1 and 2, but then gradually declined in the caudal direction with significantly lower levels in slices 6 to 15 than in slice 4 (Fig. 5a). Likewise, DA turnover as indicated by the molar ratio of HVA to DA almost linearly decreased from rostral to caudal with ratios correlating with slice numbers (correlation coefficient of 0.96, $p < 0.001$) and a significantly negative slope ($p < 0.001$) (Fig. 5a). In the PUT, HVA levels initially increased in its most rostral part parallel with significantly higher levels in slice 6 than slice 3, but then dramatically declined in the caudal direction with significantly lower levels in slices 9–12 than in slice 6 as analyzed by Friedman Repeated Measures Analysis of Variance on Ranks (Fig. 5b). Thus, highest levels of DA were associated with lowest levels of HVA.

Interestingly, the caudal part of the PUT with its increasing levels of DA was associated with a contrasting decay in its turnover with the molar ratio of HVA to DA displaying a rostro-caudal linear gradient with ratios correlating with slice numbers (correlation coefficient of 0.98, $p < 0.001$) and a significantly negative slope ($p < 0.001$) (Fig. 5b). We next analyzed whether in the medio-lateral and dorso-ventral direction levels of HVA follow the pattern of DA concentrations. In contrast to DA levels of HVA were lower in the intermediate part of the CN as compared to the lateral one (significant in slice 6 and 7; Fig. 2b, left). Medial and dorsal parts had the lowest HVA levels (slices 2–8 and 3–5, respectively). In the CN the high DA levels in the intermediate parts were associated with comparatively low HVA/DA ratios being significantly lower than in ventral

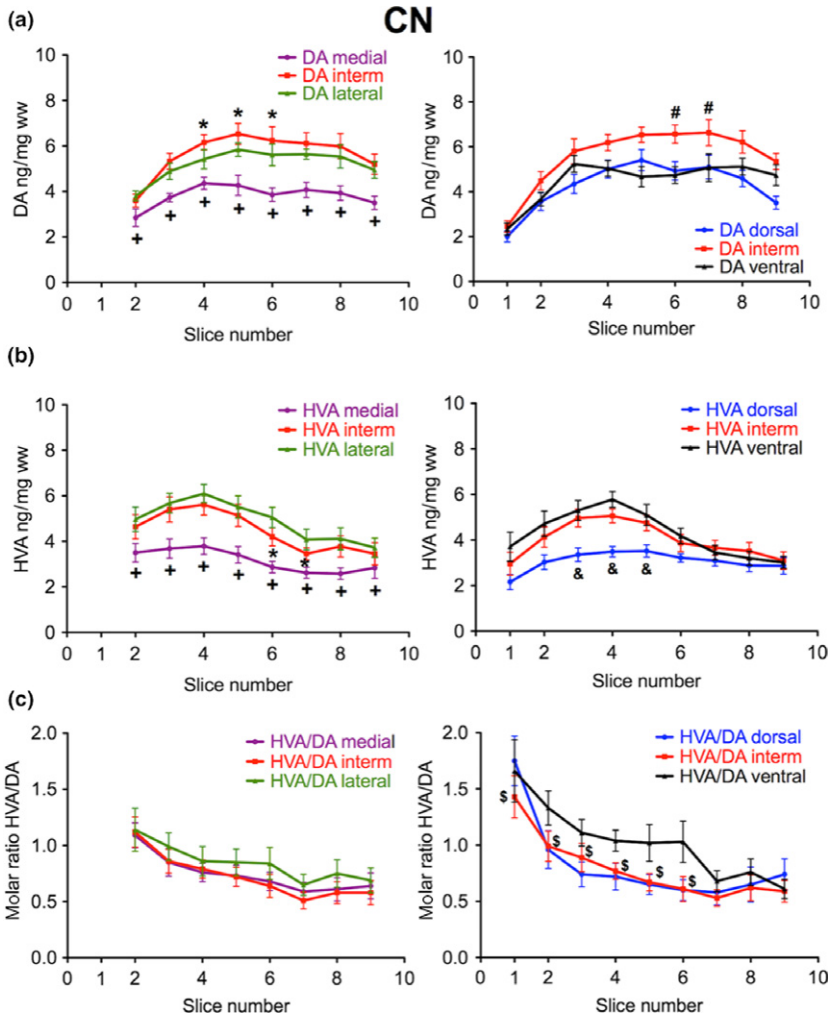

Fig. 2 Subregional distribution of DA and HVA in the human CN along the rostro-caudal gradient from slices 2 to 9. (a) The concentration of DA in ng/mg ww is presented in the medial (purple), intermediate (red), and lateral (green) third (left; number of brains = 6) as well as in the dorsal (blue), intermediate (red) and ventral (black) third (right; number of brains = 10). $^{*}p < 0.05$ versus medial and lateral; $+p < 0.05$ versus intermediate and lateral; $\#p < 0.05$ versus dorsal and ventral. (b) The concentration of HVA in ng/mg ww is presented in the medial (purple), intermediate (red), and lateral (green) third (left; number of brains = 6) as well as in the dorsal (blue), intermediate (red), and ventral (black) third (right; number of brains = 10); $^{*}p < 0.05$ versus medial and lateral; $+p < 0.05$ versus intermediate and lateral; $\#p < 0.05$ versus ventral and dorsal; $\&p < 0.05$ versus intermediate and ventral. (c) The corresponding molar ratio of HVA to DA is indicated from medial to lateral (left) and dorsal to ventral (right); $\$p < 0.05$ intermediate vs. ventral. The data are given as mean ± SEM.

parts (slices 1 to 6; see Fig. 2c). In the PUT HVA levels initially increased in the most rostral part, but then gradually declined in all subregions with significantly lower levels in slices 11 and 12 than in slice 6 (Fig. 3b). HVA/DA ratios were not significantly different from other subregions in the DA-rich intermediate parts (Fig. 3c). Moreover, the high DA content of the central area was associated with a low molar HVA/DA ratio both in CN and PUT (Fig. 4b).

In the human striatum DOPAC is a minor metabolite. DOPAC levels and likewise the molar ratios of DOPAC/DA were considerably lower (40–50 times) than HVA levels and molar ratios of HVA/DA, both in the CN and PUT (Figure S2). DOPAC levels and the molar ratio of DOPAC/DA declined in the rostro-caudal direction both in the CN and PUT comparable to the decline of HVA and the molar ratio of HVA/DA.

Age dependence of the distribution of dopaminergic parameters in the human striatum

Next we analyzed whether the distribution and concentration of DA and HVA changes depended on the age of the subject (Fig. 6). Although the number in each age segment (38–48 years, 57-66 years and 70–81 years) was small (n = 3–4) it was obvious that DA levels were considerably lower in the oldest subjects both in the CN (significantly in slices 2–14) and the PUT (significantly in slices 6–10). In the oldest subjects we observed no significant rostro-caudal DA gradient in the CN and in the PUT (Fig. 6a). DA levels (and gradients) did not differ between the ages 38–48 years or 57–66 years. In the oldest subjects lower DA levels in the PUT were paralleled by increased HVA levels. In the CN we observed no significant differences in HVA levels between ages (Fig. 6b). HVA/DA ratios, however, were significantly higher in the CN (slices 6–9) and throughout the PUT (notably in slices 7–12) of the oldest group (Fig. 6c).

Differences in the rostro-caudal distribution of choline acetyltransferase in the human putamen and caudate nucleus

We next focused on the rostro-caudal distribution of ChAT activity as a marker for the cholinergic innervation (Fig. 7; for presentation of respective box-plots see Figure S1b).

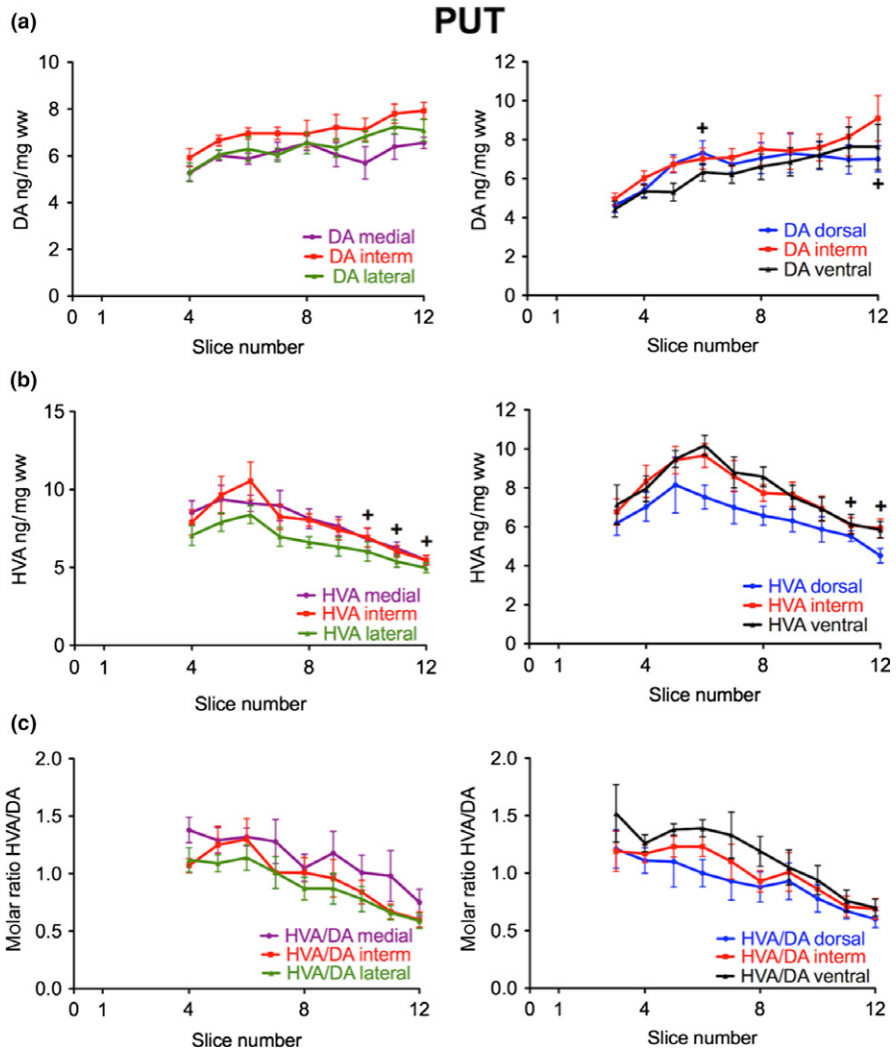

Fig. 3 Subregional distribution of DA and HVA in the human PUT along the rostro-caudal gradient. (a) The concentration of DA in ng/mg ww is presented in the medial (purple), intermediate (red), and lateral (green) third (left; number of brains = 6) as well as in the dorsal (blue), intermediate (red), and ventral (black) third (right; number of brains = 10); $+p < 0.05$ slices 6 and 12 versus slice 3 of dorsal PUT. (b) The concentration of HVA in ng/mg ww is presented in the medial (purple), intermediate (red), and lateral (green) third (left; number of brains = 6) as well as in the dorsal (blue), intermediate (red), and ventral (black) third (right; number of brains = 10); $+p < 0.05$ versus slice 6 in all subregions. (c) The corresponding molar ratio of HVA to DA is indicated from medial to lateral (left) and dorsal to ventral (right). The data are given as mean ± SEM.

Similarly to DA ChAT activity was higher in the PUT than in the CN throughout the whole nucleus with significant higher values in slices 4–12. Interestingly, the activity of the enzyme somehow followed the rostro-caudal gradient of DA, both in the PUT and CN (Fig. 7a, compared to Fig. 1a): increasing levels correlating linearly with slice numbers in the PUT with a correlation coefficient of 0.94 ($p < 0.001$) and a significantly positive slope ($p < 0.001$) and a maximum in the CN at slice 10 with significantly higher activity than in slices 1 and 15. When analyzing the subregions in medio-lateral and dorso-ventral direction we observed uneven distribution. However, in contrast to DA, the activity of ChAT was not highest in the intermediate parts, neither of the CN nor of the PUT (Figure S3). The lowest ChAT activities were detected in the medial parts of the CN and of the PUT, lower than in intermediate and lateral parts of all slices. In ventral parts ChAT activity was lower than in intermediate and dorsal parts seen only in caudal slices of the CN and some rostral slices of the PUT (Figure S3a and b). In contrast to DA, ChAT activity was not higher in the most central parts (see Fig. 7b).

Distribution of serotonergic and GABAergic markers in the human striatum

Next, we were interested whether serotonergic and GABAergic parameters also show similar concentration gradients as

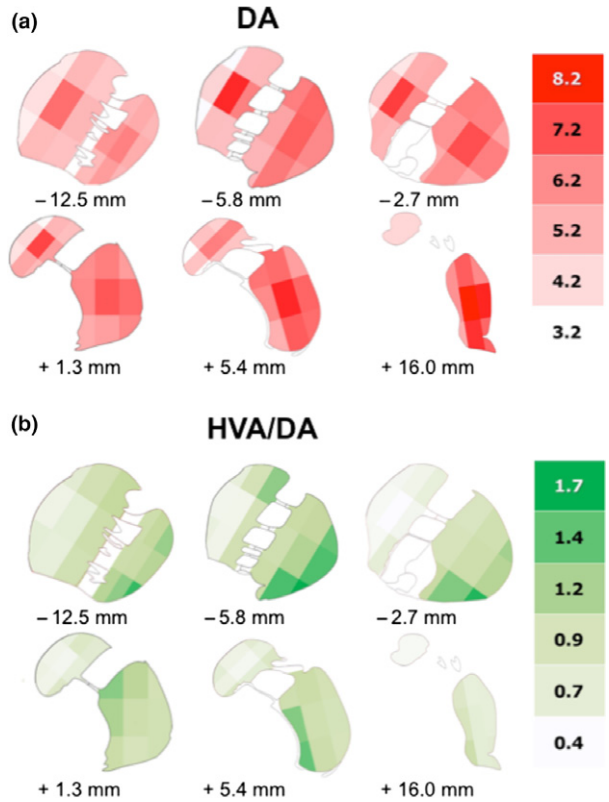

Fig. 4 Detailed distribution of DA and the molar ratio of HVA to DA in the human CN and PUT. (a) Detailed distribution of DA in the human CN and PUT as shown in six representative slices of the human striatum. In each coronal section the areas of CN and PUT were subdivided into nine parts. The schematic drawing indicates the varying concentrations of DA (ng/mg ww) within CN and PUT (number of brains = 7). (b) Detailed distribution of the molar ratio of HVA to DA (HVA/DA) in the human CN and PUT as shown in six representative slices of the human dorsal striatum. In each coronal section the areas of CN and PUT were subdivided into nine parts. The schematic drawing indicates the varying ratios of HVA/DA within CN and PUT (number of brains = 6).

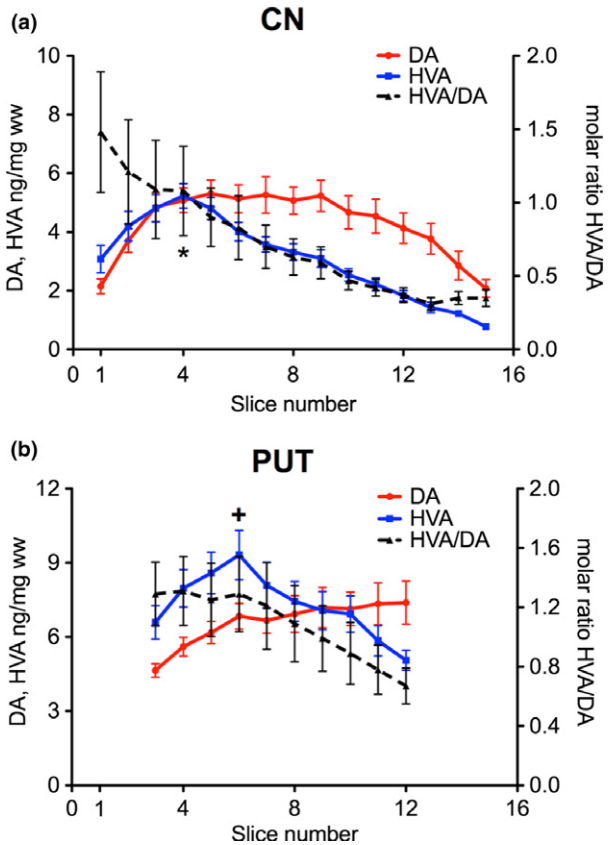

Fig. 5 Rostro-caudal gradients of DA (red), HVA (blue) and the molar ratio of HVA/DA (dashed line) in the human CN (a) and PUT (b); $^{*}p < 0.05$ of HVA in slice 4 versus slices 1 and 2 and slices 6-15 of CN; $+p < 0.05$ of HVA in slice 6 versus slice 3 and slices 9-12 of PUT. The data are given as mean ± SEM (number of brains = 10). The molar ratio of HVA/DA decreased from rostral to caudal with a correlation coefficient of 0.96 and 0.98 ($p < 0.001$) in the CN and PUT, respectively, and a significantly negative slope ($p < 0.001$) both in CN and PUT.

DA. For this purpose, we analyzed the levels of 5-HT and its metabolite 5-HIAA as well as the levels of GABA (Fig. 8). In the CN a rather even rostro-caudal distribution of 5-HT and 5-HIAA was found with a slight decrease in the caudal portions of the intermediate and ventral subdivisions (significantly lower 5-HT levels in slices 8 and 9 than in slice 4); the lowest levels were present in the dorsal portions (significantly lower in slices 1, 3, and 4; Fig. 8a, left panel) In contrast to DA, the concentrations of 5-HT and 5-HIAA were not highest in the intermediate part. Similarly, in all subdivisions of the PUT 5-HT levels slightly decreased from rostral to caudal (Fig. 8b, left panel). Interestingly, the 5-HIAA concentrations subsided in the most rostral part of the PUT (Fig. 8b, right panel), contrasting the increase in HVA in the same specimens (see Fig. 3b). Concerning the levels of GABA a distribution similar to that of 5-HT was observed in the CN (significantly lower levels in slices 8 and 9 than slice 2 in intermediate and ventral but not in dorsal subdivision; Fig. 8c left). In the PUT, GABA levels increased in the most rostral parts, especially in the ventral subdivision (Fig. 8c, right). This increase in GABA in the rostral part of the PUT parallels that of HVA. In contrast to DA the levels of GABA were not highest in the most central part (see Figure S4).

Correlation of neurotransmitter parameters over the rostro-caudal slices

Based on the distinct rostro-caudal gradients of the neurotransmitter parameters and their metabolites, we analyzed our data for possible correlations between DA and 5-HT markers of afferent striatal neurons and neurotransmitter markers of intrinsic striatal neurons GABA or ChAT. Interestingly, a high correlation was observed for the molar 5-HIAA/5-HT

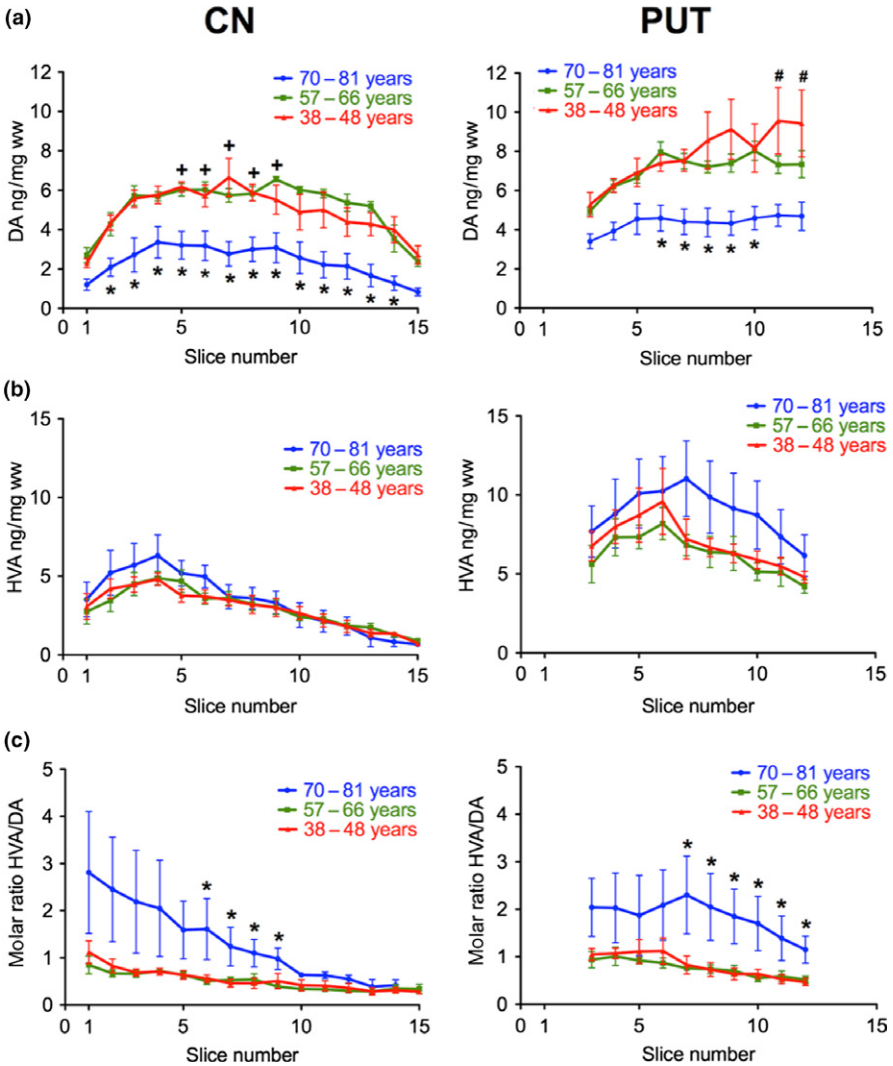

Fig. 6 Age-dependence of the levels of DA and HVA and the molar ratio of HVA/DA along the rostro-caudal gradient of the human CN and PUT. (a) Rostro-caudal gradients of the concentrations of DA are shown in three different age groups: 38–48 years (red; number of brains = 4), 57–66 years (green; number of brains = 4), and 70–81 years (blue; number of brains = 3); *$p < 0.05$ versus 38–48 and 57–66 years; +$p < 0.05$ versus slice 1 and 15 in 38–48 and 57–66 years. #$p < 0.05$ in 38–48 years versus slice 3. (b) Rostro-caudal gradients of the concentrations of HVA are shown in the three age groups. (c) Rostro-caudal gradients of the ratio of HVA/DA are shown in three different age groups. *$p < 0.05$ versus 38-48 and 57–66 years. The data are given as mean ± SEM.

ratios (an indicator of 5-HT turnover) with GABA levels in the ventral CN (correlation coefficient 0.961, $p = 0.000139$; Figure S5). A correlation of these parameters was, however, not detected in any other striatal subregion. In contrast a negative correlation, also significant after Bonferroni correction for repetitive calculations, was found between HVA/DA ratios and ChAT activity in the medial PUT (correlation coefficient −0.917, $p = 0.000492$). This negative correlation, although with lower significance, was also present in all other subregions of the PUT (dorsal PUT: $p = 0.0073$; intermediate PUT: $p = 0.00437$; ventral PUT: $p = 0.000987$; lateral PUT: $p = 0.00248$).

Discussion

This study provides a detailed mapping of the distribution of various neuronal markers in the human CN and PUT. Each neuronal marker has a distinct distribution pattern, differing between CN and PUT. Moreover, one striking result we obtained is that all neuronal parameters measured revealed higher levels, turnover or activities in the PUT as compared to the CN (e.g. see Fig. 1, Fig. 7a or Fig. 8).

Subregional levels of the neurotransmitter marker DA and 5-HT may represent differences in the innervation of respective aminergic neurons. To some extent, they could

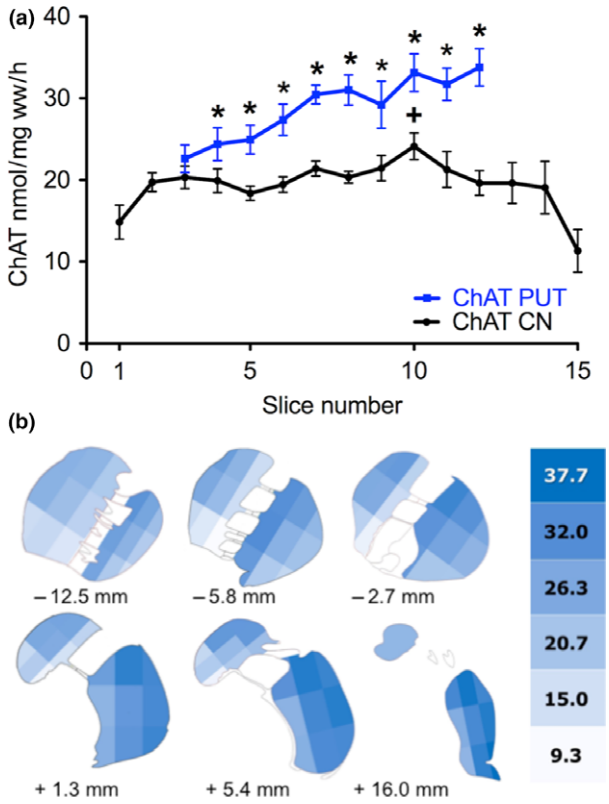

Fig. 7 Detailed distribution of ChAT activity as marker for cholinergic neurons in the human CN and PUT. (a) Rostro-caudal gradient of ChAT activity as marker for cholinergic neurons in the human CN and PUT. (a) ChAT activity (nmol/mg ww/h) was calculated as the average activity for the whole area of CN (black) and PUT (red) within the corresponding slice (number of brains = 5). The rostro-caudal gradients very much resemble those of DA both in the CN and the PUT (see Fig. 1a); $^{*}p < 0.05$ versus CN; $+p < 0.05$ versus slice 1 and 15; see Fig. S1B for presentation of respective box-plots). In the PUT ChAT increased from rostral to caudal with correlation coefficients of 0.94 ($p < 0.001$) and a significantly positive slope ($p < 0.001$). (b) Detailed distribution of ChAT activity in the human CN and PUT as shown in six representative slices of the human striatum. In each coronal section the area of CN and PUT were subdivided into nine parts. The schematic drawing indicates the varying activities of ChAT (nmol/ mg ww/h) within CN and PUT (number of brains = 5).

of course also reflect differences in the number of aminergic vesicles contained per nerve terminal. Molar ratios of HVA/DA and of 5-HIAA/5-HT may reflect the amount of transmitter release per aminergic terminal, thus may be a rough measure for the turnover or, that is, activity of the respective aminergic nerve terminal. According to Eisenhofer *et al.* (2004) most of this metabolism occurs independently of exocytotic release. Differences in GABA levels and ChAT activity may also reflect differences in the densities (to some extent also activities) of the respective neurons within the striatum.

Distribution patterns of dopaminergic markers

A remarkable finding is the continuous increase in DA concentrations from rostral to caudal in the PUT. This increasing gradient was not observed in the CN. In contrast, in the body of the CN, DA levels gradually declined in the caudal direction. These rostro-caudal gradients very well agree with the rostro-caudal gradients observed for striatal $DA_{2,3}$ receptor binding in the living healthy human brain (Alakurtti *et al.* 2013). In the CN, the initial increase in the receptor binding in the most rostral part of the CN head, followed by a decreasing gradient in the caudal direction convincingly agrees with the gradient of DA levels in the CN observed in this study and reported previously (Kish *et al.* 1988). Similarly, DA concentrations increasing rostro-caudally in the PUT very well match the same gradient of $DA_{2,3}$ receptor binding *in vivo* (Alakurtti *et al.* 2013). According to Piggott et al. (1999) the increasing rostro-caudal gradient of DA_2 receptors binding in the PUT is contrasted by a rostro-caudally declining gradient of DA_1 receptor binding.

The DA levels and their rostro-caudal gradients observed by us do not, however, agree with those described by Piggott et al. (1999). These authors reported even lower levels of DA in the PUT as compared to the CN and a decline in the caudal part of both nuclei. A possible explanation for this discrepancy is the fact that the brains investigated by Piggott et al. (1999) were obtained from subjects with a mean age of 77.2 years and a mean *post-mortem* delay of 36.1 h, very different to the mean age of 60.5 years and the *post-mortem* delay of 11.4 h in our study. This explanation is supported by the age dependence of DA levels demonstrated in this study. It highlights a marked decrease in DA in the age group of 70–81 years both in the CN and PUT and a loss in respective transmitter gradients (see Fig. 6a). This specific pattern of striatal DA loss with increasing age has also been shown by Kish *et al.* (1992).

It is also remarkable that both in the PUT and the CN the highest DA levels were seen in the most central area of each slice (see Fig. 4a). This specific distribution was characteristic for DA throughout the rostro-caudal gradient. In contrast, the molar ratio of HVA/DA was lower in the central part as compared to the surrounding areas (Fig. 4b). This indicates that the areas with the highest DA levels are associated with a low DA turnover. The specific distribution of DA was not observed for any of the other neuronal parameters analyzed in our study (for ChAT see Fig. 7b, for GABA see Figure S4).

Concerning the metabolism of DA we showed that in the PUT the highest levels of DA were associated with the lowest levels of HVA. The decrease in the molar ratios of HVA/DA in the caudal parts of the PUT may be related to a decrease in the release of DA, possibly as a consequence of the higher $DA_{2,3}$ receptor binding described by Alakurtti *et al.* (2013). In both striatal nuclei the molar ratio of HVA to DA steadily declined from rostral to caudal. This is additionally confirmed by the rostro-caudal gradients of DOPAC and DOPAC/DA.

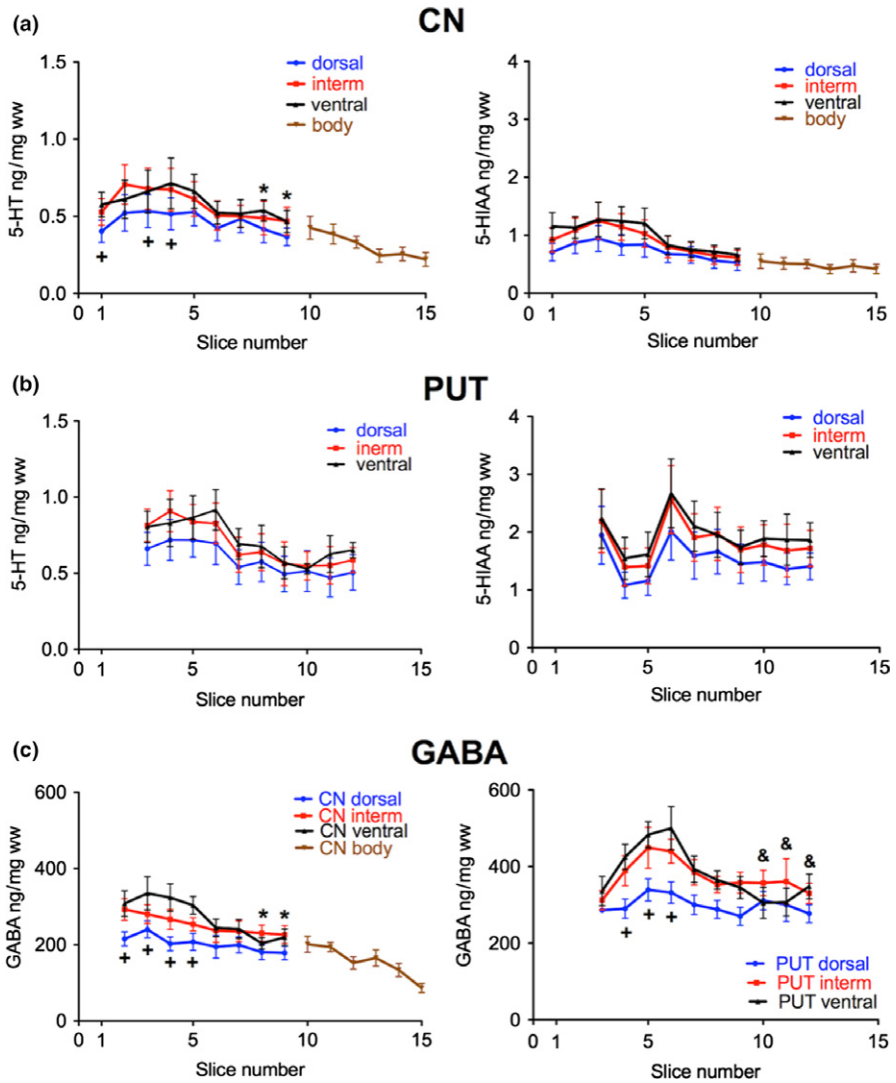

Fig. 8 Subregional distribution of 5-HT, 5-hydroxyindoleacetic acid (5-HIAA), and γ-aminobuturic acid (GABA) in the human CN and PUT along the rostro-caudal gradient. (a) The concentrations of 5-HT and 5-HIAA in ww is presented in the dorsal (blue), intermediate (red), and ventral (black) third of the CN (number of brains = 7); *$p < 0.05$ versus slice 4 of intermediate and ventral CN; +$p < 0.05$ versus intermediate and ventral. (b) The concentrations of 5-HT and 5-HIAA in ng/mg ww is presented in the dorsal (blue), intermediate (red), and ventral (black) third of the PUT (number of brains = 5). (c) The concentrations of GABA in ng/mg ww is presented in the dorsal (blue), intermediate (red), and ventral (black) third of the CN (left; number of brains = 7–9) and of the PUT (right; number of brains = 7–9). +$p < 0.05$ versus intermediate and ventral; *$p < 0.05$ versus slice 2 of intermediate and ventral CN; &$p < 0.05$ versus slices 5 and 6 of ventral PUT. The data are given as mean ± SEM.

According to Jarbo and Verstynen (2015) motor and somatosensory cortical areas tend to terminate in more caudal regions of the striatum, especially in the caudal PUT. These projections coincide with the high DA content in this specific striatal area.

Changes of dopaminergic markers in the diseased striatum and during aging

The divergence of the rostro-caudal gradients of DA and its metabolites is of special interest since in Parkinson's disease the most pronounced loss of DA occurs in the caudal portion of the PUT (Kish *et al.* 1988). In healthy brains it contains the highest DA concentrations associated with the lowest HVA/DA ratios indicating lower DA turnover in these areas (see Fig. 5). In addition, DA transporter uptake was significantly decreased in the Parkinsonian striatum with the greatest loss in the posterior PUT (Wang *et al.* 2006). In patients with *de novo* Parkinson's disease elevated molar HVA/DA ratios in the caudal portions of the PUT, though not in the CN is associated with an increased risk for later

motor complications (Löhle *et al.* 2015). Similarly, in Huntington's disease the caudal portion of the PUT is more degenerated than the rostral portion in the early phase of the disease (Vonsattel and DiFiglia 1998). Our findings exclude that a high turnover rate may contribute to the degeneration of dopaminergic neurons.

In this respect it may be of interest that we found a remarkable loss of DA in the age group of 70 years and older, especially in the PUT of neurologically healthy subjects: It was accompanied by higher levels of HVA and higher HVA/DA ratios as compared to younger subjects (see Fig. 6c) This is in good agreement to previous findings (Kish *et al.* 1992). These findings indicate that the loss of dopaminergic projections in elderly persons may be partially compensated by increased DA release from the remaining dopaminergic nerve endings. As compared to subjects aged 38–66 years the decrease of DA was obvious along the rostro-caudal gradient, both in the CN and the PUT of the oldest group (70–81 years). The age-dependent loss of DA was comparable in PUT and CN of neurologically healthy subjects, but it was different to the pattern of DA losses in Parkinson's disease. In patients with idiopathic Parkinson's disease the most pronounced DA deficits are present in the caudal PUT and to a much milder degree in the CN, especially in its caudal portion (Kish *et al.* 1988). These findings together with those of Kish *et al.* (1992) indicate a clear difference in the loss of DA in normal aging and the dopaminergic neurodegeneration in Parkinson's disease.

Distribution patterns of cholinergic markers

With regards to the cholinergic interneurons, Bernácer *et al.* (2007) demonstrated a clear differential distribution of ChAT immunoreactivity in the distinct topographical and functional territories of the human dorsal striatum. They demonstrated that the CN is more densely populated by cholinergic neurons than the PUT and that the CN body contains the highest density of ChAT neurons of the whole striatum. In contrast to the distribution of cholinergic neurons, we found higher ChAT activities in the PUT as compared to those in the CN. Moreover, in the CN body with its highest density of cholinergic interneurons the activity of ChAT was lowest and gradually declined in the rostro-caudal direction. On the other hand, in the PUT the number of immunoreactive cholinergic interneurons increases from precommissural to postcommissural territories (Bernácer *et al.* 2007) in agreement with the rostro-caudal increase in the ChAT activity in this area.

In most striatal territories, the distribution of cholinergic interneurons follows a decreasing dorso-ventral gradient (Bernácer *et al.* 2007). Similarly, we also observed a decreasing dorso-ventral gradient in ChAT activity both in the CN and PUT. According to Bernácer *et al.* (2007) the volume of the perikarya of the cholinergic cells also varies between the different striatal territories. The variation in the volume might be related to the variation in density indicating that the increase in size reflects the need to compensate for the lack of higher neuronal density (Bernácer *et al.* 2007). In this study, the highest activities of ChAT were measured in the territories of lowest densities of cholinergic interneurons (i.e. PUT), and lowest activities in areas of high density (i.e. CN body). These differences clearly indicate that cholinergic activity is not only determined by the number of cholinergic neurons but also by the activity of the acetylcholine synthesizing enzyme. A unique feature in the human striatum is that the dense ChAT immunostaining is found mainly in the matrix of the dorsal CN and dorso-medial PUT (Holt *et al.* 1996). Remarkably, thalamostriatal projections have a strong impact on cholinergic interneurons (for review see Yamanaka *et al.* 2018).

The negative correlation between DA turnover and ChAT activity in all subregions of the PUT might reflect a tonic inhibition of cholinergic neurons by the dopaminergic input, since blockade of D2 receptors has been reported to stimulate acetylcholine release (Damsma *et al.,* 1990; Bertorelli and Consolo, 1990; Marien and Richard, 1990). However, dopamine D2 receptor agonists inhibited striatal acetylcholine release in microdialysis studies in the striatum of conscious rats (Damsma *et al.,* 1990; Bertorelli and Consolo, 1990; Stoof *et al.,* 1992).

Distribution patterns of serotoninergic and GABAergic markers

The lower levels of 5-HT in the CN are in agreement with the slightly weaker 5-HT innervation of the CN as compared to that of the PUT (Wallman *et al.* 2011). The dorso-ventral gradient of 5-HT in CN and PUT parallels the previously described clear dorso-ventral gradient of 5-HT immunopositive axon profiles being more abundant ventrally than dorsally (Wallman *et al.* 2011). The observed lower 5-HIAA levels in the most rostral part of the PUT are contrasted by higher HVA in this part of the PUT and may indicate that the 5-HT release is slowed down by higher dopaminergic activity. On the other hand, a positive correlation between molar 5-HIAA/5-HT ratios and GABA levels might be because of the inhibitory action of 5-HT on GABA release via 5-HT1B receptors increasing GABA tissue levels (Nishijo and Momiyama, 2016; Momiyama and Nishijo, 2017), which, based on our subregional analysis, seems to be only active in the ventral CN.

In the rostral part of the PUT, GABA levels increase parallel to DA and HVA, especially in the ventral extension. Although GABA is mainly contained in interneurons and projection neurons arising from the dorsal striatum, it has to be considered that GABA may also act as a co-transmitter in dopaminergic nigrostriatal projections, as suggested by animal studies (Tritsch *et al.,* 2012; Kim *et al.* 2015; for review see Chuhma *et al.* 2017). Therefore it cannot be excluded that GABA derived from dopaminergic neurons contributes to the GABA levels measured, especially in the rostral part of the PUT.

In conclusion, our data demonstrate a highly diverse but specific distribution of neurotransmitter markers in the human dorsal striatum indicating diverse innervation and functional activity of the respective neurons and neuronal circuitries. This considerable diversity in the concentration of neurotransmitter markers as well as in their turnover rates within the striatum must also be taken into account, when comparing tissue samples from healthy and diseased striatum.

Acknowledgments and conflict of interest disclosure

Prof. Dr. Oleh Hornykiewicz deserves our special thanks and appreciation for initiating this specific study and for his brilliant dissection of the human striatum samples. We thank Elisabeth Schlögel-Hanslik and Harald Reither for skilful and excellent technical assistance. This work was supported by the Medical University of Vienna. The authors declare no conflict of interest.

Supporting information

Additional supporting information may be found online in the Supporting Information section at the end of the article.

Figure S1. Box-plots presentation of the rostro-caudal gradients of DA and ChAT activity in the CN and PUT.

Figure S2. Subregional distribution of DOPAC and the molar ratio of DOPAC/DA in the human CN and PUT along the rostro-caudal gradient.

Figure S3. The subregional distribution of ChAT activity in the human striatum.

Figure S4. Distribution of GABA in the human striatum.

Figure S5. Correlation of 5-HT turnover and GABA in the human striatum.

Table S1. Actual DA values ± SEM schematically presented in Fig. 4.

References

Alakurtti K., Johansson J. J., Tuokkola T., Nagren K. and Rinne J. O. (2013) Rostrocaudal gradients of dopamine $D_{2/3}$ receptor binding in striatal subregions measured with {^{11}C}raclopride and high-resolution positron emission tomography. *NeuroImage* **82**, 252–259.

Bernácer J., Prensa L. and Giménez-Amaya J. M. (2007) Cholinergic interneurons are differentially distributed in the human striatum. *PLoS ONE* **11**, e1174.

Bertorelli R. and Consolo S. (1990) D1 and D2 dopaminergic regulation of acetylcholine release from striata of freely moving rats. *J. Neurochem.* **54**, 2145–2148.

Chuhma N., Mingote S., Kalmbach A., Yetnikoff L. and Rayport S. (2017) Heterogeneity in dopamine neuron synaptic actions across the stzriatum and its relevance for schizophrenia. *Biol. Psychiatry* **81**, 43–51.

Crittenden J. R. and Graybiel A. M. (2011) Basal ganglia disorders associated with imbalances in the striatal striosome and matrix compartments. *Front. Neuroanat.* **5**, 59.

Damsma G., de Boer P., Westerink B. H. and Fibiger H. C. (1990) Dopaminergic regulation of striatal cholinergic interneurons: an in vivo microdialysis study. *Naunyn Schmiedebergs Arch. Pharmacol.* **342**, 523–527.

Ebinger G., Michotte Y. and Herregodts P. (1987) The significance of homovanillic acid and 3,4-dihydroxyphenylacetic acid concentrations in human lumbar cerebrospinal fluid. *J. Neurochem.* **48**, 1725–1729.

Eisenhofer G., Kopin I. J. and Goldstein D. S. (2004) Catecholamine metabolism: A contemporary view with implications for physiology and medicine. *Pharmacol. Reviews* **56**, 331–349.

Felice L. J., Felice J. D. and Kissinger P. T. (1978) Determination of catecholamines in rat brain parts by reversed phase ion-pair liquid chromatography. *J. Neurochem.* **31**, 1461–1465.

Fonnum F. (1969) Radiochemical microassay for determination of choline actyltransferase and acetylcholinesterase activities. *Biochem. J.* **115**, 465–472.

Goto S., Hirano A. and Matsumoto S. (1989) Subdivisional involvement of nigrostriatal loop in idiopathic Parkinson's disease and striatonigral degeneration. *Ann. Neurol.* **26**, 766–770.

Graybiel A. M. (1990) Neurotransmitters and neuromodulators in the basal ganglia. *Trends Neurosc.* **13**, 244–254.

Graybiel A. M. and Ragsdale C. W., Jr (1978) Histochemically distinct compartments in the striatum of human, monkey, and cat demonstratedby acetylcholinesterase staining. *Proc. Natl Acad. Sci. USA* **75**, 5723–5726.

Holt D. J., Hersh L. B. and Saper C. B. (1996) Cholinergic innervation in the human striatum: A three-compartment model. *Neuroscience* **74**, 67–87.

Hong J. Y., Oh J. S., Lee I., Sunwoo M. K., Ham J. H., Lee J. E., Sohn Y. H., Kim J. S. and Lee P. H. (2014) Presynaptic dopamine depletion predicts levodopa-induced dyskinesia in de novo Parkinson disease. *Neurology* **82**, 1597–1604.

Jarbo K. and Verstynen T. D. (2015) Converging structural and functional connectivity of orbifrontal, dorsolateral prefrontal, and posterior parietal cortex in the human striatum. *J. Neuroscience* **35**, 3865–3878.

Johnston J. G., Gerfen C. R., Haber S. N. and van der Kooye D. (1990) Mechanisms of striatal pattern formation: conservation of mammalian compartmentalization. *Dev. Brain Res.* **57**, 93–102.

Kim J.-I., Ganesan S., Luo S. X., Wu Y.-W., Park E., Huang E. J., Chen L. and Ding J. B. (2015) Aldehyde dehydrogenase 1a1 mediates a GABA synthesis pathway in midbrain dopaminergic neurons. *Science* **350**, 102–106.

Kish S. J., Shannak K. and Hornykiewicz O. (1988) Uneven pattern of dopamine loss in the striatum of patients with idiopathic Parkinson's disease. *N. Engl. J. Med.* **318**, 876–880.

Kish S. J., Shannak K., Rajput A., Deck J. H. and Hornykiewicz O. (1992) Aging produces a specific pattern of striatal dopamine loss: implications for the etiology of idiopathic Parkinson's disease. *J. Neurochem.* **58**, 642–648.

Kopin I. J. (1985) Catecholamine metabolism: basic aspects and clinical significance. *Pharmacol. Reviews* **37**, 333–364.

Kotz S. A., Anwender A., Axer H. and Knösche T. R. (2013) Beyond Cytoarchitectonics: The Internal and external connectivity structure of the caudate nucleus. *PLoS ONE* **8**, e70741.

Löhle M., Mende J., Wolz M., Beuthien-Baumann B., Oehme L., van den Hoff J., Kotzerke J., Reichmann H. and Storch A. (2015) Putaminal dopamine turnover in de novo Parkinson disease predicts later motor complications. *Neurology* **86**, 231–240.

Mai J. K., Assheuer J. and Paxinos G. (1997) *Atlas of the human brain*. Academic Press, Harcourt Brace & Company, San Diego, London, Boston, New York, Sidney, Tokyo, Toronto.

Marien M. R. and Richard J. W. (1990) Drug effects on the release of endogenous acetylcholine in vivo: measurement by intracerebral dialysis and gas chromatography-mass spectrometry. *J. Neurochem.* **54**, 2016–2023.

Momiyama T. and Nishijo T. (2017) Dopamine and Serotonin-Induced Modulation of GABAergic and Glutamatergic Transmission in the Striatum and Basal Forebrain. *Front. Neuroanat.* **11**, 42.

Morigaki R. and Goto S. (2016) Putaminal mosaic visualized by tyrosine hydroxlase immunohistochemistry in the human neostriatum. *Front. Neuroanat.* **10**, 34.

Morrish P. K., Sawle G. V. and Brooks D. J. (1996) Regional changes in {18F}dopa metabolism in the striatum in Parkinson's disease. *Brain* **119**, 2097–2103.

Nishijo T. and Momiyama T. (2016) Serotonin 5-HT1B receptor-mediated calcium influx-independent presynaptic inhibition of GABA release onto rat basal forebrain cholinergic neurons. *Eur. J. Neurosci.* **44**, 1747–1760.

Parkes L., Fulcher B. D., Yücel M. and Fornito A. (2017) Transcriptional signatures of connectomic subregions of the human striatum. *Genes, Brain Behavior.* **16**, 647–663.

Piggott M. A., Marshall E. F., Thomas N., Lloyd S., Court J. A., Jaros E., Costa D., Perry R. H. and Perry E. K. (1999) Dopaminergic activities in the human striatum: rostrocaudal gradients of uptake sites and of D_1 and D_2 bur not od D_3 receptor binding or dopamine. *Neuroscience* **92**, 433–445.

Riley H. A. (1960) *An Atlas of the Basal Ganglia, Brainstem and Spinal Cord*. Hafner Publishing, New York.

Schmid R., Hong J. S., Meek J. and Costa E. (1980) The effect of kainic acid on the hippocampal content of putative transmitter amino acids. *Brain Res.* **200**, 355–362.

Shipp S. (2017) The functional logic of corticostriatal connections. *Brain Struct Funct.* **222**, 669–706.

Sperk G. (1982) Simultaneous determination of serotonin, 5-hydroxyindoleacetic acid, 3,4-dihydroxyphenylaceticacid and homovanillic acid by high performance liquid chromatography with electrochemical detection. *J. Neurochem.* **38**, 840–843.

Sperk G., Berger M., Hörtnagl H. and Homykiewicz O. (1981) Kainic acid- induced changes of serotonin and dopamine metabolism in the striaturn and substantia nigra of the rat. *Eur. J. Pharmacol.* **74**, 279–286.

Sperk G., Lassmann H., Baran H., Kish S. J., Seitelberger F. and Homykiewicz O. (1983) Kainic acid induced seizures: neurochemical and histopathological changes. *Neuroscience* **10**, 1301–1315.

Stoof J. C., Drukarch B., de Boer P., Westerink B. H. and Groenewegen H. J. (1992) Regulation of the activity of striatal cholinergic neurons by dopamine. *Neuroscience* **47**, 755–770.

Tritsch N. X., Ding J. B. and Sabatini B. L. (2012) Dopaminergic neurons inhibit striatal output through non-canonical release of GABA. *Nature* **490**, 262–266.

Vonsattel J.-P. G. and DiFiglia M. (1998) Huntington Disease. *J. Neuropathol. Exp. Neurol.* **57**, 369–384.

Wallman M.-J., Gagnon D. and Parent M. (2011) Serotonin innervation of human basal ganglia. *Eur. J. Neurosci.* **33**, 1519–1532.

Wang J., Zuo C.-T., Jiang Y.-P., Guan Z.-P., Xiang J.-D., Yang L.-Q., Ding Z.-T., Wu J.-J. and Su H.-L. (2006) ^{18}F-FP-CIT PET imaging and SPM analysis of dopamine transporters in Parkinson's disease in various Hoehn & Yahr stages. *J. Neurol.* **254**, 185–190.

Widmann R. and Sperk G. (1986) Topographical distribution of amines and major amine metabolites in the rat striatum. *Brain Res.* **367**, 244–249.

Wilk S. and Stanley M. (1978) Dopamine metabolites in human brain. *Psychopharmacology* **57**, 77–81.

Yamanaka K., Hori Y., Minamimoto T., Yamada H., Matsumoto N., Enomoto K., Aosaki T., Graybiel A. M. and Kimura M. (2018) Roles of centromedian parafascicular nuclei of thalamus and cholinergic interneurons in the dorsal striatum in associative learning of environmental events. *J. Neural. Transm.* **125**, 501–513.

